JOC The Journal of Organic Chemistry

pubs.acs.org/joc Article

Peculiar Reaction Products and Mechanisms Revisited with Machine Learning-Augmented Computational NMR

Ivan M. Novitskiy and Andrei G. Kutateladze*

Cite This: J. Org. Chem. 2022, 87, 8589−8598 Read Online

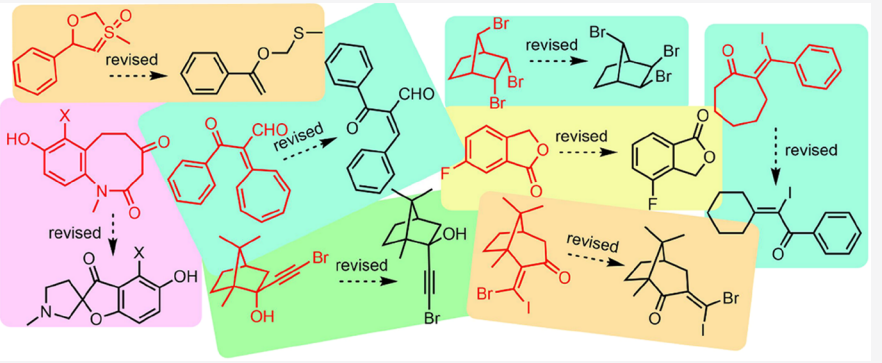

ABSTRACT: DU8ML, a fast and accurate machine learning-augmented density functional theory (DFT) method for computing nuclear magnetic resonance (NMR) spectra, proved effective for high-throughput revision of misassigned natural products. In this paper, we disclose another important aspect of its application: correction of unusual reaction mechanisms originally proposed because of incorrect product structures.

INTRODUCTION

Structure elucidation of products of chemical reactions plays a very special role in chemical sciences, including mechanistic organic chemistry. Self-evidently, a sensible mechanistic rationale must account for the observed products, and that is where things get complicated if the structures of reaction products are misassigned. Nuclear magnetic resonance (NMR), as the most informative analytical tool for solution structure elucidation, is clearly experiencing a renaissance due to significant advances in novel pulse sequences and multidimensional experiments.[1] Concurrently, computational NMR has matured and become user-friendly to a point that it is more and more broadly used by the practitioners in the field as a routine tool. This is true for both *ab initio*/density functional theory (DFT) methods[2] and a group of computer-aided structure elucidators, CASEs, which normally rely on fast neural network algorithms but also are increasingly utilizing DFT.[3] While such calculations are more commonly used to support structure elucidation of natural products, they are also used in assigning structures of synthetic products.[4]

We have developed a machine learning-augmented DFT method for computational NMR, DU8ML,[5] which proved fast and accurate in revisions of many important natural products. Our approach is to "label" the substructure fragments, responsible for major deviations of the DFT-calculated values, with the appropriate SMARTS strings[6] and train the machine on a large set of reliable experimental nuclear spin coupling constants and chemical shifts to recognize the discrepancies and correct them. In 2014, we expanded on Bally and Rablen's idea[7] of scaling Fermi contacts and developed a fast and accurate method for computing nuclear spin−spin coupling constants based on a substructure-aware scaling.[8] Later, we applied a similar methodology for calculations of chemical shifts.[9] Most notably, for molecules containing heavy atoms, e.g., halogens, this pragmatic approach circumvented the need to deploy expensive spin−orbit coupling, SOC, calculations. All in all, DU8ML together with its predecessor DU8+ accounted for hundreds of revised structures.[10]

In this work, we discuss the important role of DU8ML in helping to avoid incorrect mechanistic inferences based on the erroneous interpretation of the product structure. In short, we examined unusual reactions and reaction products reported in the literature and found a number of flawed reaction mechanisms put forward because of inaccurate structure elucidation work.

Received: March 31, 2022
Published: June 18, 2022

https://doi.org/10.1021/acs.joc.2c00749
J. Org. Chem. 2022, 87, 8589−8598

RESULTS AND DISCUSSION

Figure 1A shows a recent report of water-mediated intramolecular cyclization/oxidation of α-carbonyl sulfur ylides for

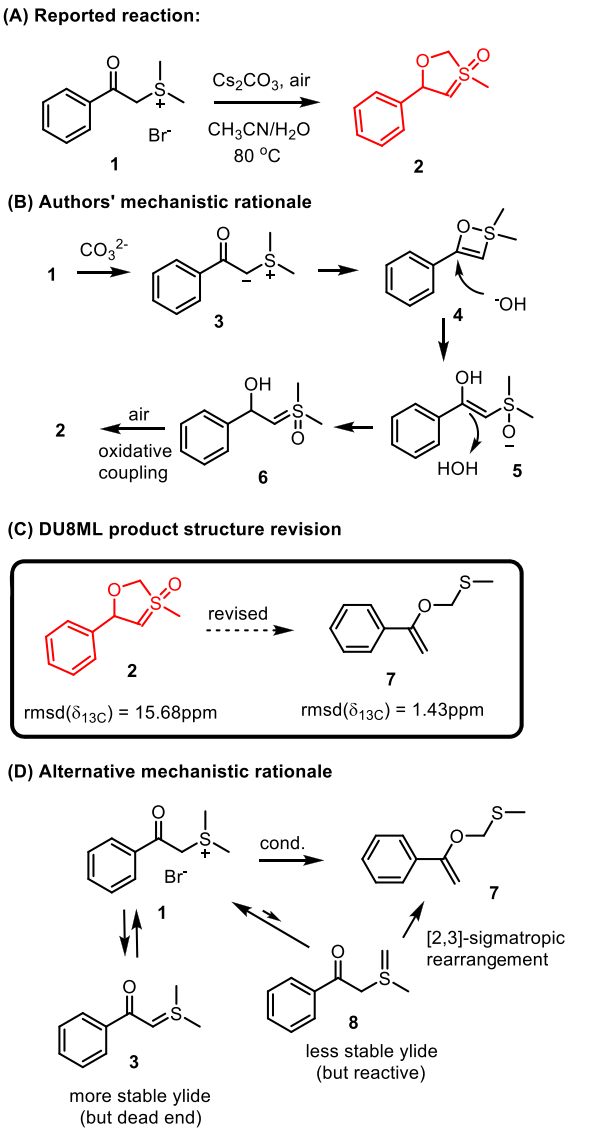

Figure 1. Reported formation of cyclic Corey–Chaykovsky-type ylides and DU8ML-driven revision.

the synthesis of Corey–Chaykovsky reagent-like heterocycles.[11] The authors evaluated the scope of this reaction, presenting a large table of 24 products. However, both the peculiar product structure and the unusual original mechanistic rationale—including the postulated oxathiete **4**, its odd ring opening, protonation, and subsequent oxidative coupling of the Corey–Chaykovsky intermediate **6** into the cyclic Corey–Chaykovsky product **2**—raised reasonable questions. DU8ML revealed irreconcilable differences between the calculated and experimental ^{13}C chemical shifts for **2**. At the same time, product **7** of a 2,3-sigmatropic shift in the less stable ylide **8** (Figure 1D) matched the experimental NMR. We therefore revised product **2** to the shown 2-(methylthiomethoxy)styrene **7**. The 2,3-sigmatropic rearrangement of ylides derived from **1** and similar sulfonium salts was described by Ratts and Yao,[12] with ^{13}C NMR of **7**—matching the experimental spectrum of **2**—later reported by Russell.[13] This leaves no doubts that the Corey–Chaykovsky heterocycles shown in Figure 1 are erroneous.

Another recent example of an unusual photocatalyzed dehydroxylative amination of hydroquinones with 4-piperidones, sensitized by iron phthalocyanine, is shown in Figure 2.[14] The reaction was purported to occur via a ring expansion

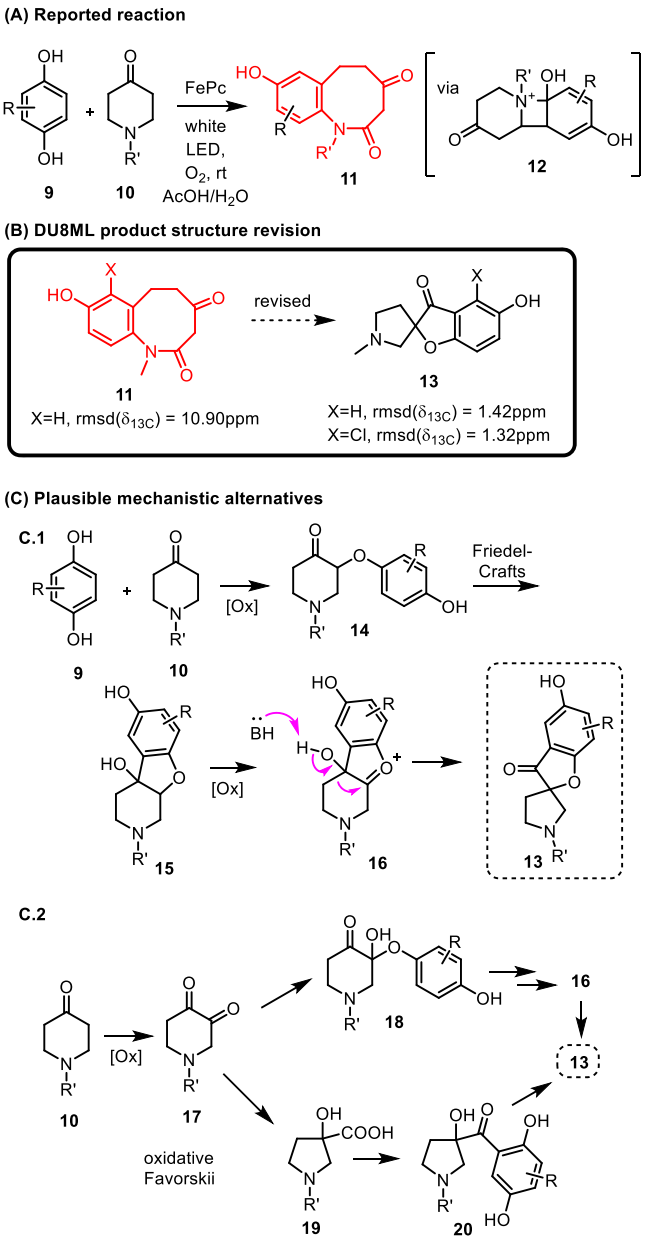

Figure 2. Revision of the proposed benzoazocine structure and plausible mechanistic alternatives.

route and produce eight-membered benzolactam products **11**. Its scope was found to be rather general, as evidenced by 30 examples. The proposed complex mechanistic rationale necessitated two azetidine intermediates, for example, **12**.

DU8ML computations showed a very poor match for the computed and experimental ^{13}C chemical shifts, rmsd (δ_{13C}) = 10.9 ppm, clearly indicative of misassignment. The search for revision led us to spiro-pyrrolidines **13**, which best matched the experimental NMR data. Substituted benzofuranones

https://doi.org/10.1021/acs.joc.2c00749
J. Org. Chem. 2022, 87, 8589–8598

spiro-connected to pyrrolidines are known and could potentially have useful pharmacological properties.[15]

A number of plausible reaction mechanisms for the formation of spiro-benzofuranones **13** could be suggested. One of them, involving the well-precedented[16] oxidative coupling of phenols with enolizable ketones as a first step to form intermediate **14**, is shown in Figure 2 (C.1). Subsequent intermolecular Friedel–Crafts reaction is followed by additional oxidative steps furnishing oxonium ion **16** and setting up the final pinacol–pinacolone rearrangement to arrive at spiro-product **13**.

Yet another alternative route, mechanism C.2, could involve the formation of α-diketone **17**, which reacts with substituted hydroquinones to form hemiacetal **18** and then proceeds through the Friedel–Crafts step and pinacol–pinacolone rearrangement via **16** to give **13** or, in another variant, be involved in the (precedented) oxidative Favorskii-type reaction[17] leading to **19** with subsequent ground-state transformations to furnish **13**.

It is unlikely that the tertiary amine moiety is redox-active in the context of these reactions because it should be fully protonated by excess acetic acid. The regiochemistry of oxidation in N-acyl piperidones into position 3 is also precedented in the literature.[18] Generally, one wonders if other cyclic—and not necessarily heterocyclic—ketones could be utilized in this photoinduced reaction to expand the scope.

DDQ was used in another oxidative coupling reaction between cycloheptatriene and benzoylenamines **21**, reportedly furnishing 2-cycloheptatrienylidene-3-oxo-3-phenylpropanal **23** (Figure 3).[19] The scope was confirmed by 15 additional

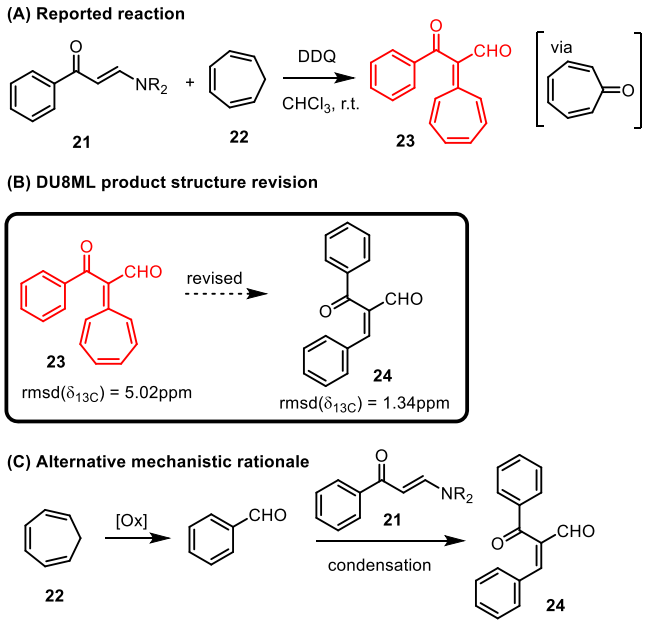

Figure 3. Revision of the oxidative coupling between cycloheptatriene and enamine **17**.

examples. As a similar reaction was reported for xanthenes,[20] with one of the products confirmed by X-ray crystallography, the formation of **23** in a reaction with cycloheptatriene therefore did not raise any red flags. However, the ^{1}H NMR spectrum of **23**, in addition to the formyl singlet, clearly had another unexplained broad singlet in the aromatic region of the spectrum.

A closer inspection of the spectral data indicated that **23** has what appears to be two phenyl groups. DU8ML computations rejected the cycloheptatrienylidene structure and helped arrive at a Z-benzylidene product **24**. Obviously, the revised product has the same chemical formula and the same exact mass. Our mechanistic rationale is based on a precedented oxidative transformation of cyclohexatriene into benzaldehyde, for example, when reacted with hypervalent iodine reagents.[21] It appears that this oxidative rearrangement in the described DDQ reaction produces sufficient amounts of benzaldehyde for condensation with enamine **21**. The Z-configuration of the product is confirmed computationally: rmsd (δ_{13C}) = 1.34 ppm, while for the E-isomer (not shown), the match is degraded to rmsd (δ_{13C}) = 2.48 ppm.

A somewhat counterintuitive mechanistic rationale was proposed for the bromination reaction of benzoquinone-fused norbornadiene **25** (Figure 4).[22] Stereochemical analysis

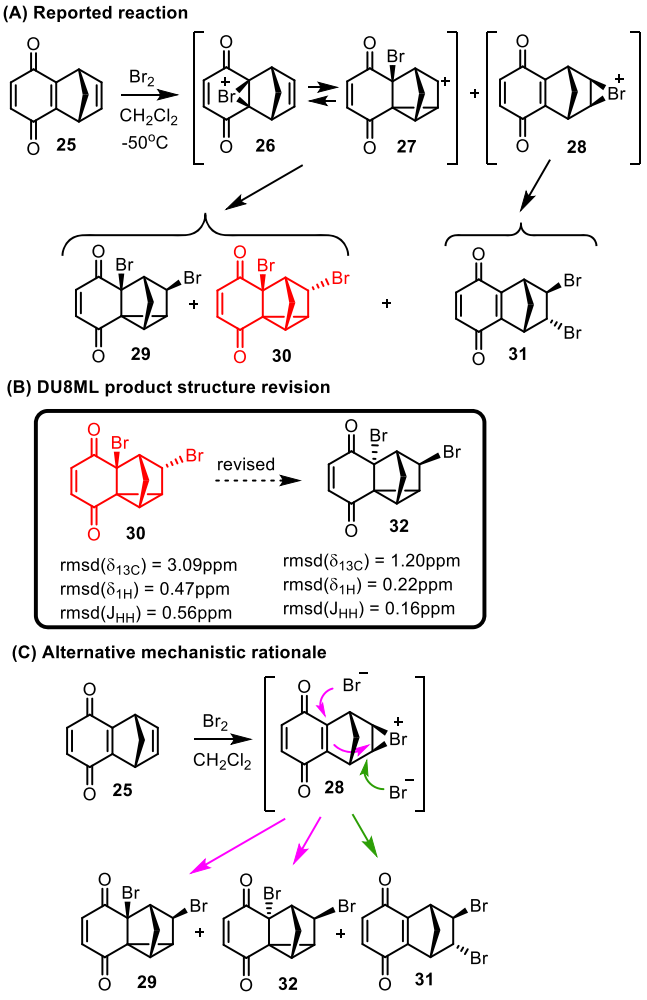

Figure 4. Revision of the stereoconfiguration of product **30** and streamlining of the mechanism of low-temperature bromination of benzoquinone-fused norbornadiene **25**.

of the three products, **29**, **30**, and **31**, i.e., the only products obtained at low temperature, −50 °C or lower, produced a hypothesis that the 1,2-dibromide, **31** is formed from bromonium ion **28**, while the 1,3-dibromides, **29** and **30**, were derived from an alternative bromonium ion **26** (or its nortricyclene form **27**).

https://doi.org/10.1021/acs.joc.2c00749
J. Org. Chem. 2022, 87, 8589−8598

The discrepancy was that the ratio of products **31** to (**29** + **30**) was ~2:1, while the authors' DFT computations found bromonium ion **26** to be 3.5 kcal/mol higher in energy than the more stable bromonium **28**. Unless some unforeseen kinetic control was operational, these two facts were hard to reconcile. This dilemma was resolved with DU8ML revealing that the stereochemistry of 1,3-dibromide **30** was misassigned. It is revised to the shown bis-epimer **32**. This structure revision allowed for a simpler mechanistic rationale presented in Figure 4C, where the sole most stable bromonium ion **28** is responsible for all products observed at low temperature. In fact, none of the products observed in the low- or high-temperature experiments necessitate bromonium ion **26** on the reaction coordinate.

Another bromination study in the *syn*-7-bromonorbornene series produced a number of tribromonorbornanes and dibromonortricyclenes.[23] Most of them were rationalized in terms of the *exo*-bromonium intermediate **38** (Figure 5).

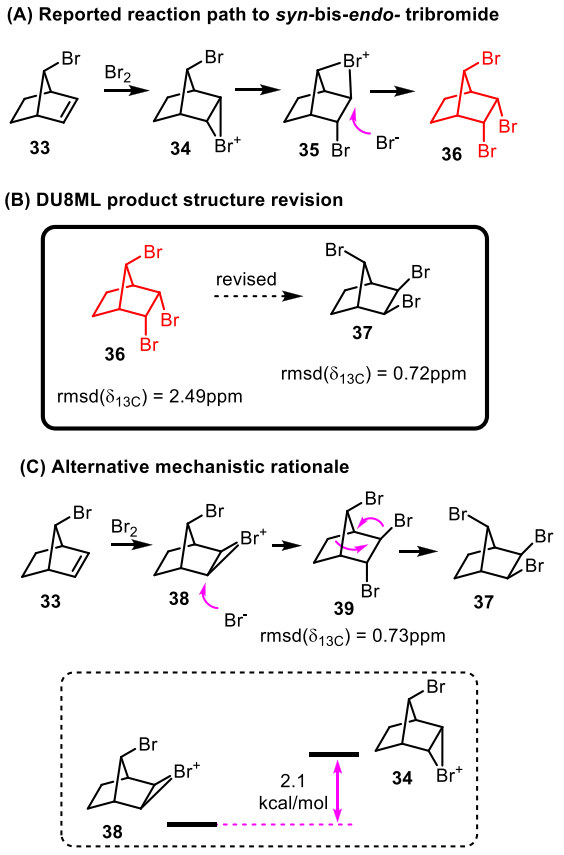

Figure 5. Bromination of *syn*-bromonorbornene.

However, one product—tribromide **36**—was derived from the *endo*-bromonium species **34**, rearranging into a four-membered bromonium **35**. This prompted us to verify the structure of **36**. DU8ML-calculated chemical shifts were inconsistent with the experimental data for **36**, and it was revised to another C_s-symmetric *anti*-7-bis-*exo*-tribromide **37**.

One plausible mechanistic rationale for its formation involves another observed (and correctly assigned, rmsd (δ_{13C}) = 0.73 ppm) tribromide **39**, which could be envisioned to undergo a concerted dyotropic[24] or stepwise Wagner–Meerwein rearrangement to yield **37**. As **39**, and other observed products, could be formed via the *exo*-bromonium cation **38**, there seem to be little evidence necessitating the *endo*-bromonium **34**, which we calculated to be >2 kcal/mol uphill of **38**.

A detailed study of aerobic dehydrogenative α-oxygenation of ethers with an iron catalyst involved a broad range of substrates, including phthalans shown in Figure 6.[25] The

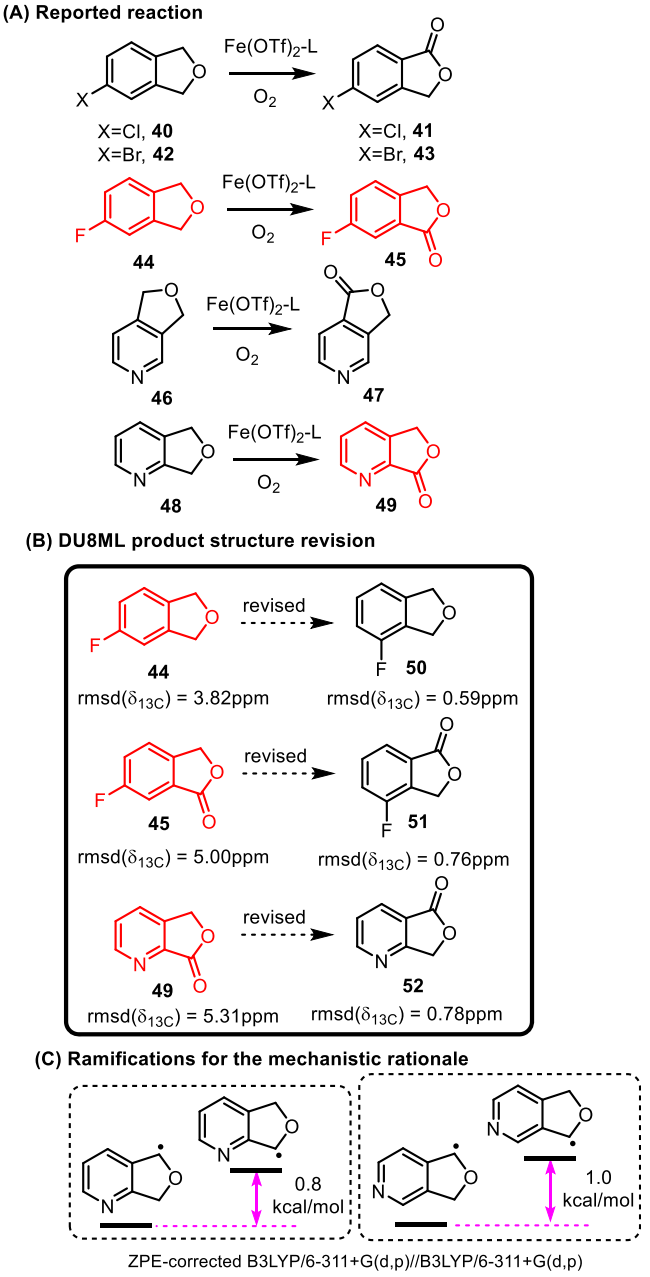

Figure 6. Aerobic oxidation of phthalans with an iron catalyst.

authors correlated the observed regiochemistry of oxidation in the halogenated dihydroisobenzofuran series with "a strong meta-directing effect" of the fluorine substituent (σ_m = 0.34 vs σ_p = 0.06) and "significantly stronger *para* directing effect (σ_m = 0.37 for Cl and 0.39 for Br vs σ_p = 0.23 for both)" for the chlorine and bromine substituents. Given the reported results with fused pyridines, this was a debatable rationale.

These reservations were partially resolved by the DU8ML analysis. First, the structures of the starting materials in the 5-halogen-1,3-dihydroisobenzofuran series—fluoro **44**, chloro

https://doi.org/10.1021/acs.joc.2c00749
J. Org. Chem. 2022, 87, 8589–8598

40, and bromo **42**—were examined and the fluoro isobenzofuran **44** required revision to 4-fluoro **50**, which was probably due to an error with the precursor of fluoride **44**.

The structures of the chloro- and bromo-substituted isobenzofurans **40** and **42** were confirmed as 5-substituted isobenzofurans (rmsds 0.79 and 0.89 ppm, respectively). Of the oxidation products, which required two structure revisions: the fluoro-isobenzofuranone **45** was revised to the *ortho* isomer **51**, and pyridine **49** needed the correction of the oxidation site (revised to **52**).[26]

Revision of the fluoro product **45** did not change the relative positions of the fluorine and the newly formed carbonyl assigned by the authors; i.e., it remained *meta*. However, the revised pyridine **52** has the carbonyl in position 3, not 2, while the correctly assigned pyridine **47** has the carbonyl in position 4. Clearly, Hammett's $\sigma_{m/p}$ argument invoked by the authors is not uniformly applicable here. Instead, as Figure 6C shows, the regiochemistry of this aerobic oxidation in pyridines may better correlate with the stability of the respective radicals. Also, the fact that **49** is revised to **52** implies that (the expected) precoordination of the iron catalyst to the pyridine's nitrogen is unlikely a factor driving the regiochemistry of the oxidation.

An extensive diepoxidation study of substituted cyclohexa-3,5-diene-1,2-diols produced enantiopure benzene dioxide intermediates (Figure 7),[27] which were further studied in the thermal valence tautomerization to 1,4-dioxocins as a racemization mechanism.

The path to the desired dioxiranes involved hydroxylation of the dienic moiety with OsO_4/Me_3NO and the Mattocks reaction[28] furnishing bromoacetates **55** or **58**, which were treated with sodium methoxide.[29] DU8ML analysis of the relative stereochemistry of the resulting diepoxy products, for which ^{13}C NMR was reported, confirmed the *syn*-diepoxide **59**, rmsd (δ_{13C}) = 0.78ppm, but pointed to a stereochemical mismatch for diepoxide **56**, which was revised to the *anti*-diastereomer **60** (relative configuration is implied).

As ^{13}C NMR data is not available for its precursor **55**, it is difficult to draw conclusions at what step the mechanistic rationale needs a revision. Curiously, the relative stereochemistry of tetraol **54** seems to be correct. A potential teaching moment here is that the Mattocks step is not stereospecific for tetraol **54**, possessing a tertiary alcohol moiety.

A number of reaction mechanisms in need of revision have proton-deficient halogenated products, which make solution structure elucidation challenging due to the (i) lack of informative proton spin coupling constants and (ii) difficult-to-calculate C−I or C−Br ^{13}C chemical shifts. DU8ML is particularly suitable for this work, as the heavy atom effects on carbon chemical shifts are evaluated parametrically with high accuracy.

There was a considerable effort in the 1990s put into understanding the reactivity of halogen electrophiles toward acetylene carbinols. Early on, McNelis, who was a principal contributor to these efforts, differentiated the two most common modes of reactivity: one being a variety of the Meyer−Schuster reaction,[30] which McNelis called a halo-Meyer−Schuster reaction[31] and which stood "in contrast with the conversion of tertiary alkynols to β-iodoenones" (Figure 8).

Still, until very recently, there is a fair amount of confusion about the products generated in related processes, and these errors are most certainly due to significant challenges of NMR

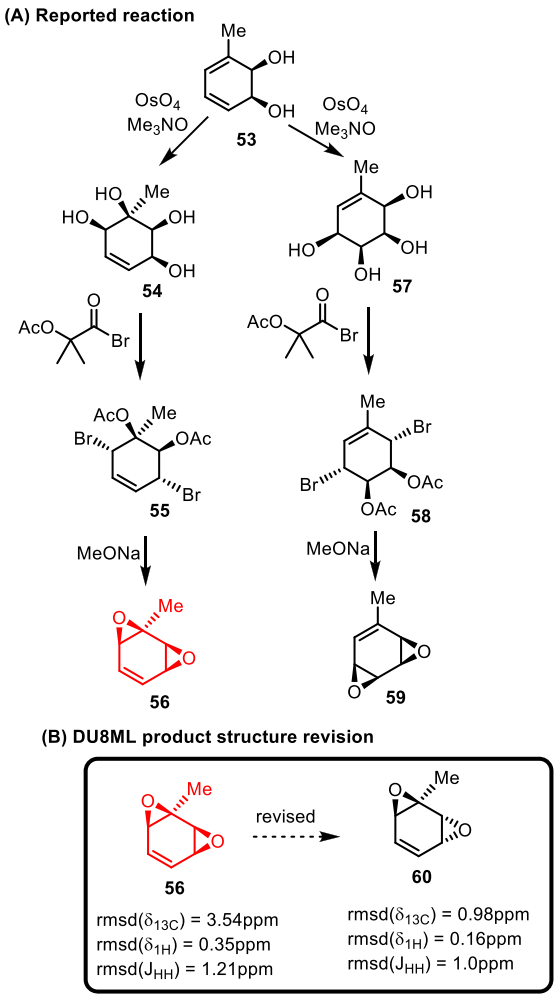

Figure 7. Diepoxidation of cyclohexa-3,5-diene-1,2-diols.

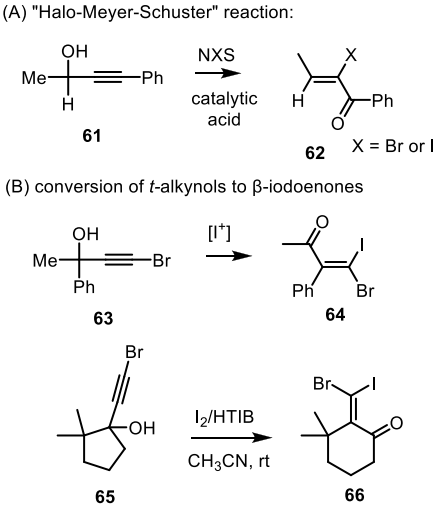

Figure 8. Two distinct reported reactivities of alkynyl carbinols in the presence of electrophilic halogen reagents.

structure elucidation of these products. For example, in a 2020 study,[32] a series of alkoxides of acetylene carbinols were synthesized and subjected to electrophilic iodination with ICl, producing the products of ring expansion **68** and **71** shown in Figure 9A.

https://doi.org/10.1021/acs.joc.2c00749
J. Org. Chem. 2022, 87, 8589−8598

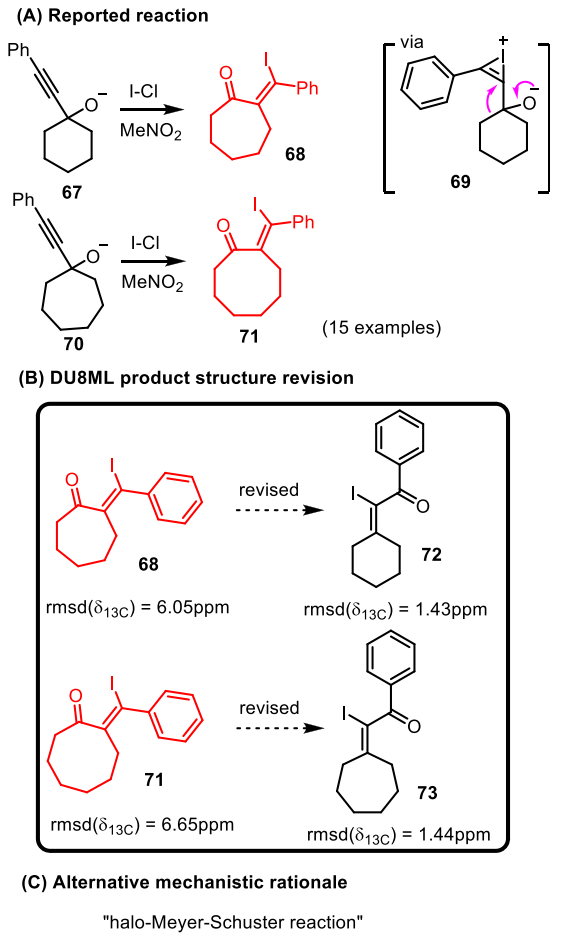

Figure 9. Halo-Meyer−Schuster reaction confused for ring expansion with the formation of *β*-iodoenones.

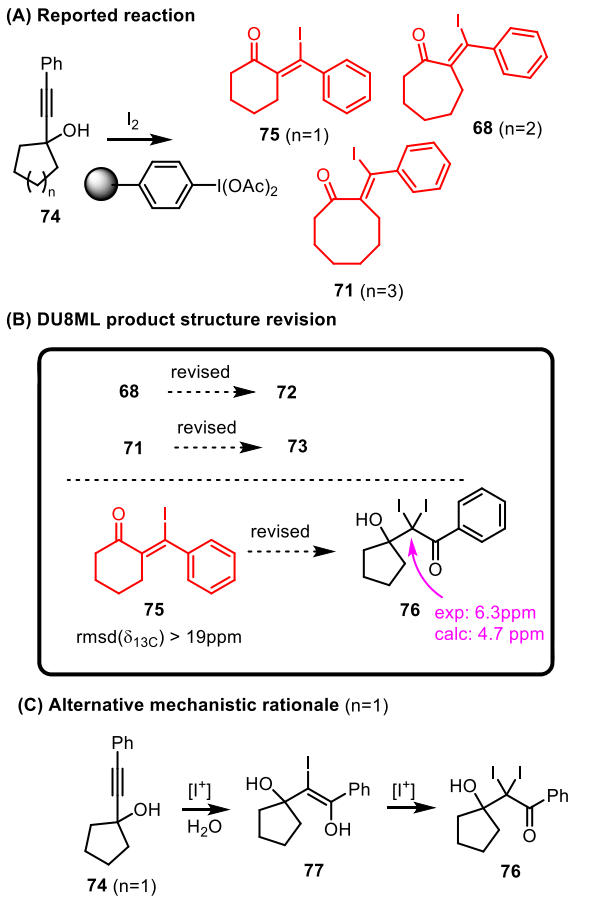

Figure 10. Similar errors in a reaction of hypervalent iodine oxidant.

The authors confirmed the generality of this reaction with 15 examples. Yet, DU8ML analysis clearly showed that the actual products **72** and **73** correspond to the halo-Meyer−Schuster reaction (Figure 9B).

A very similar reaction with I_2 and a catalytic amount of the polymer-immobilized iodine(III) reagent was published in 2004 with a similar error[33] (Figure 10); that is, for n = 2,3 instead of the purported ring expansion, the halo-Meyer−Schuster products **72** and **73** were formed. Additionally, for n = 1, under these conditions, the cyclopentanol-containing starting material did not expand the ring, as the authors suggested, and it did not undergo the halo-Meyer−Schuster rearrangement either (as the cyclohexanol and cycloheptanol congeners did).

Instead, iodination of the triple bond in the presence of water seemingly produced *α*,*α*-diiodoketone **76**, keeping the tertiary alcohol moiety intact (Figure 10). This is similar to the *α*,*α*-dibromo- and -dichloroketone formation under related conditions described earlier.[34] We could not analyze the rms deviations in this case, as the reported ^{13}C NMR spectrum contained extraneous peaks. However, one ^{13}C chemical shift in the vicinity of 6 ppm—reported for enone **75** (i.e., revised cyclopentanol **76**) and its derivatives—should have been interpreted as a clue for a potential *gem*-diiodoalkyl substitution (experimental: 6.3 ppm, calculated: 4.7 ppm).

However, the ring expansion of acetylenic carbinols does occur, most commonly—in halo-terminated acetylenes, not arylacetylenes. It was also reported[35] for more complex bicyclics, for example, acetylenic carbinols derived from camphor or norcamphor. While the majority of these studies produced correct results, the camphor-based products are misassigned, starting with the erroneous stereochemistry of the initial addition of lithium acetylenide to camphor (Figure 11). All acetylenic *endo*-carbinols derived from camphor, i.e., compounds **86**, **87**, and **88**, needed revision to *exo*-stereoisomers **91**, **92**, and **93**. The major product of the rearrangement **90** also needed revision to isomer **94**.

Mechanistic considerations offered by the authors were based on the assumption that for both camphor and norcamphor starting materials the differences in reactivity were derived solely from the nature of the migrating group (i.e., secondary carbons vs tertiary vs quaternary). The authors pointed to contrasting reactivities; i.e., for a similar cationic ring expansion in 2-N,N-dichloroaminonorbornanes[36] catalyzed by aluminum chloride, the bridgehead atom moved in the *exo*-amines, while the secondary carbon 3 migrated in the *endo*-amines. A similar trend, i.e., preferred migration of the secondary carbon in the *endo*-2-(aminomethyl)norbornane, was reported in the Demjanov rearrangement.[37]

In view of our revision of the major product **90** to isomer **94**, it appears that the ring expansion in alkynyl carbinols shown in Figure 11 does, indeed, follow the same trend determined by the stereoconfiguration of the acetylenic group, i.e., the CH_2 carbon is migrating preferably in the case of the *endo*-configuration of the acetylenic group, which is developing a carbocationic center, while the bridgehead carbon is migrating in the case of *exo*-acetylenes (Figure 11C).

https://doi.org/10.1021/acs.joc.2c00749
J. Org. Chem. 2022, 87, 8589−8598

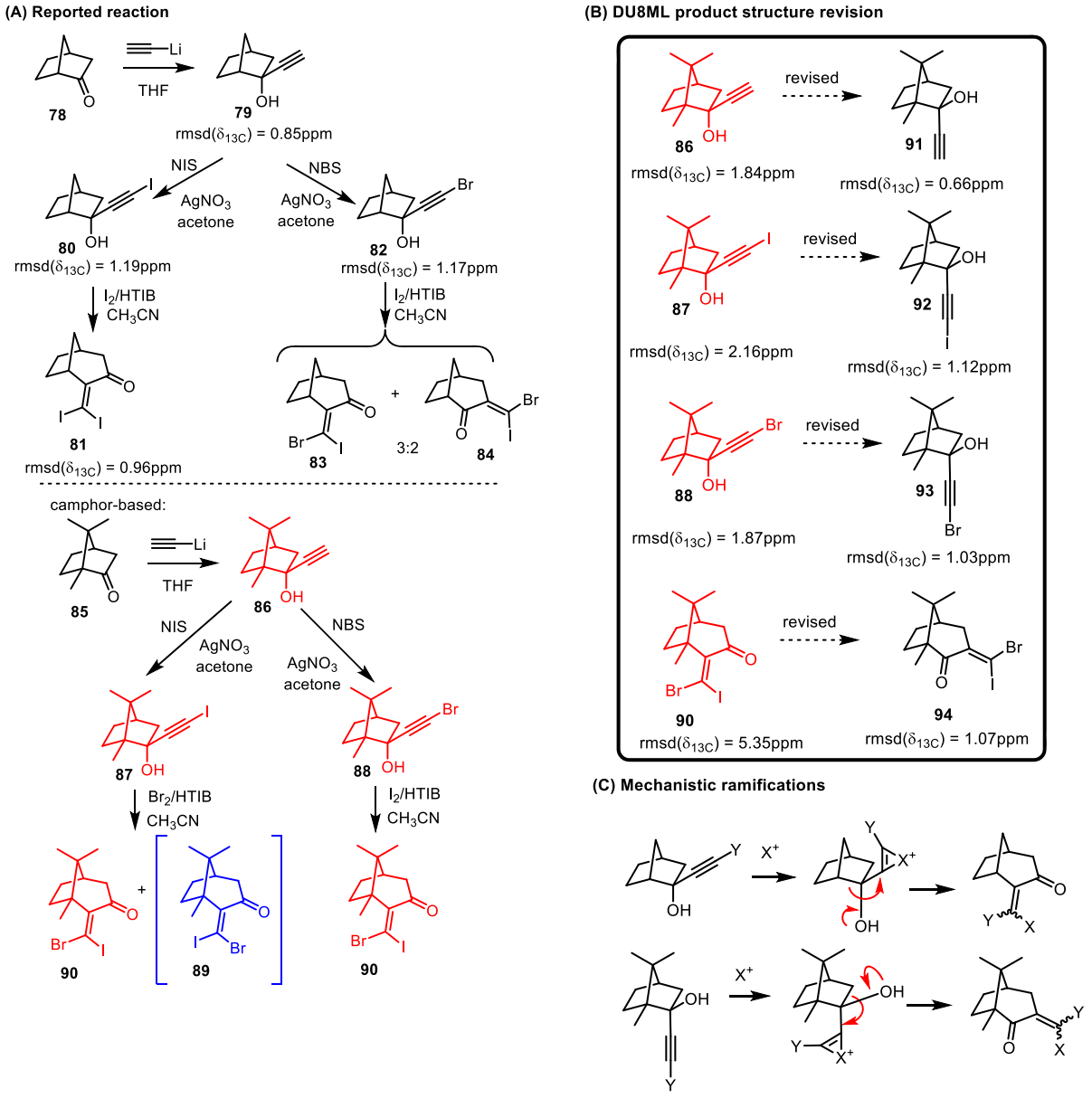

Figure 11. Ring expansion in the camphor series.

It is also important to underscore that once the erroneous stereochemistry is published, it persists in the literature; for example, the camphor-based acetylene carbinol was incorrectly assumed to be *exo* in an unrelated study.[38]

Finally, a recent isolation of diterpenoid ipomone (**96**) under acidified hydroalcoholic extract of *Ipomoea nil* seeds suggested a rearrangement path for its formation from derivatives of gibberellic acid (Figure 12).[39a] Similar rearrangement was observed with molecular iodine in methanol.[39b]

Besides the acid-induced decarboxylative aromatization of ring A, the authors focused on the pinacol−pinacolone rearrangement step to account for stereochemistry of this reaction. Yet, the reported mechanistic rationale included the formation of a questionable bridgehead carbocation and a 1,2-methyl shift, as shown in Figure 12A. Occam's razor would suggest an alternative mechanism with H^+/I^+ addition to the exocyclic double bond and subsequent migration of the in-cycle allylic carbon (Figure 12C). This mechanism requires an inverted stereochemistry of the CH_2 bridge in the bicyclo[3.2.1]octenone moiety (highlighted in cyan). DU8ML supported this hypothesis. The structure of ipomone is revised from **96** to **98**, and the structure of iodoipomone is revised from **97** to **99**.

CONCLUSIONS

Incorrectly assigned structures are problematic in countless ways. Some of them are purported to have useful properties, including beneficial biological activity. As we have shown here, very often such misassignments lead to erroneous mechanistic hypotheses, amplifying their detrimental effects on the field of organic chemistry. Luckily, solution structure elucidation by NMR is aided by substantial developments in computational NMR, including our machine learning-augmented DFT method, DU8ML. It is clear that the computational methods are now user-friendly, fast, and accurate and therefore must become an everyday tool in the toolbox of organic chemistry practitioners.

https://doi.org/10.1021/acs.joc.2c00749
J. Org. Chem. 2022, 87, 8589−8598

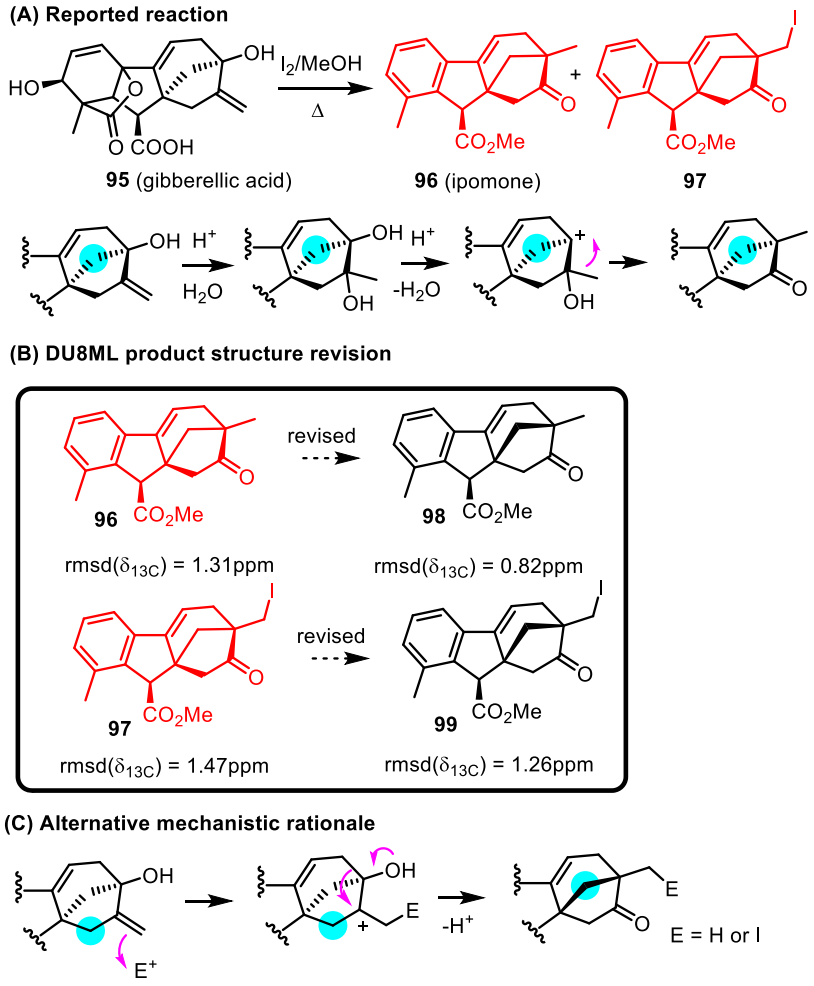

Figure 12. Revision of ipomone **96** and iodoipomone **97**.

■ ASSOCIATED CONTENT

Supporting Information

The Supporting Information is available free of charge at https://pubs.acs.org/doi/10.1021/acs.joc.2c00749.

Computational details: chemical shifts and Cartesian coordinates for computed structures (PDF)

■ AUTHOR INFORMATION

Corresponding Author

Andrei G. Kutateladze − *Department of Chemistry and Biochemistry, University of Denver, Denver, Colorado 80208, United States;* orcid.org/0000-0003-3066-517X; Email: akutatel@du.edu

Author

Ivan M. Novitskiy − *Department of Chemistry and Biochemistry, University of Denver, Denver, Colorado 80208, United States;* orcid.org/0000-0002-2675-3348

Complete contact information is available at: https://pubs.acs.org/10.1021/acs.joc.2c00749

Notes

The authors declare no competing financial interest.

■ ACKNOWLEDGMENTS

This research was supported by the NSF, CHE-1955892.

■ REFERENCES

(1) Fisher, J. *Modern NMR Techniques for Synthetic Chemistry*, CRC Press, 2021.

(2) (a) Lodewyk, M. W.; Siebert, M. R.; Tantillo, D. J. Computational Prediction of ^{1}H and ^{13}C Chemical Shifts: A Useful Tool for Natural Product, Mechanistic, and Synthetic Organic Chemistry. *Chem. Rev.* **2012**, *112*, 1839−1862. (b) See also Tantillo's excellent compilation of various NMR computational approaches at http://cheshirenmr.info (accessed 1/3/2022). (c) Marcarino, M. O.; Zanardi, M. M.; Cicetti, S.; Sarotti, A. M. NMR Calculations with Quantum Methods: Development of New Tools for Structural Elucidation and Beyond. *Acc. Chem. Res.* **2020**, *53*, 1922−1932.

(3) (a) Elyashberg, M.; Argyropoulos, D. Computer Assisted Structure Elucidation (CASE): Current and Future Perspectives. *Magn. Reson. Chem.* **2021**, *59*, 669−690. (b) Costa, F. L. P.; Albuquerque, A. C. F. de.; Fiorot, R. G.; Lião, L. M.; Martorano, L. H.; Mota, G. V. S.; Valverde, A. L.; Carneiro, J. W. M.; Junior, F. M. S. Structural Characterisation of Natural Products by Means of Quantum Chemical Calculations of NMR Parameters: New Insights. *Org. Chem. Front.* **2021**, *8*, 2019−2058. (c) Guan, Y.; Sowndarya, S. V. S.; Gallegos, L. C.; St John, P. C.; Paton, R. S. Real-time prediction of ^{1}H and ^{13}C chemical shifts with DFT accuracy using a 3D graph neural network. *Chem. Sci.* **2021**, *12*, 12012−12026. (d) Buevich, A. V.; Elyashberg, M. E. Enhancing Computer-Assisted Structure Elucidation with DFT Analysis of J-Couplings. *Magn. Reson. Chem.* **2020**, *58*, 594−606. (e) Koos, M. R. M.; Navarro-Vázquez, A.; Anklin, C.; Gil, R. R. Computer-Assisted 3D Structure Elucidation (CASE-3D): The Structural Value of 2JCH in Addition to 3JCH Coupling

Constants. *Angew. Chem., Int. Ed.* **2020**, *59*, 3938−3941. (f) Elyashberg, M. E.; Williams, A. J.; Martin, G. E. Computer-Assisted Structure Verification and Elucidation Tools in NMR-Based Structure Elucidation. *Prog. Nucl. Magn. Reson. Spectrosc.* **2008**, *53*, 1−104. (g) Elyashberg, M.; Williams, A. J.; Blinov, K. Structural Revisions of Natural Products by Computer-Assisted Structure Elucidation (CASE) Systems. *Nat. Prod. Rep.* **2010**, *27*, 1296−1328. (h) Reher, R.; Kim, H. W.; Zhang, C.; Mao, H. H.; Wang, M.; Nothias, L.-F.; Caraballo-Rodriguez, A. M.; Glukhov, E.; Teke, B.; Leao, T.; Alexander, K. L.; Duggan, B. M.; Van Everbroeck, E. L.; Dorrestein, P. C.; Cottrell, G. W.; Gerwick, W. H. A Convolutional Neural Network-Based Approach for the Rapid Annotation of Molecularly Diverse Natural Products. *J. Am. Chem. Soc.* **2020**, *142*, 4114−4120.

(4) (a) Michels, T. D.; Dowling, M. S.; Vanderwal, C. D. A Synthesis of Echinopine B. *Angew. Chem., Int. Ed.* **2012**, *51*, 7572−7576. (b) Lebeuf, R.; Robert, F.; Landais, Y. Unexpected ring contraction of 1-aryl-cyclohexa-2,5-dienes under palladium catalysis. *ARKIVOC* **2014**, *3*, 6−17. (c) Andrew, K. G.; Spivey, A. C. Improving the Accuracy of Computed ^{13}C NMR Shift Predictions by Specific Environment. *J. Org. Chem.* **2013**, *78*, 11302−11317.

(5) Novitskiy, I. M.; Kutateladze, A. G. DU8ML: Machine Learning-Augmented DFT NMR Computations for High-Throughput *in Silico* Solution Structure Validation and Revision of Complex Alkaloids. *J. Org. Chem.* **2022**, *87*, 4818−4828.

(6) https://www.daylight.com/dayhtml/doc/theory/theory.smarts.html (accessed 1/3/2022).

(7) Bally, T.; Rablen, P. R. Quantum-Chemical Simulation of ^{1}H NMR Spectra. 2. Comparison of DFT-Based Procedures for Computing Proton−Proton Coupling Constants in Organic Molecules. *J. Org. Chem.* **2011**, *76*, 4818−4830.

(8) (a) Kutateladze, A. G.; Mukhina, O. A. Relativistic Force Field: Parametric Computations of Proton−Proton Coupling Constants in ^{1}H NMR Spectra. *J. Org. Chem.* **2014**, *79*, 8397−8406. (b) Kutateladze, A. G.; Mukhina, O. A. Relativistic Force Field: Parametrization of ^{13}C−^{1}H Nuclear Spin−Spin Coupling Constants. *J. Org. Chem.* **2015**, *80*, 10838−10848.

(9) Kutateladze, A. G.; Reddy, D. S. High-Throughput in Silico Structure Validation and Revision of Halogenated Natural Products Is Enabled by Parametric Corrections to DFT-Computed ^{13}C NMR Chemical Shifts and Spin−Spin Coupling Constants. *J. Org. Chem.* **2017**, *82*, 3368−3381.

(10) (a) Kutateladze, A. G.; Kuznetsov, D. M.; Beloglazkina, A. A.; Holt, T. Addressing the Challenges of Structure Elucidation in Natural Products Possessing the Oxirane Moiety. *J. Org. Chem.* **2018**, *83*, 8341−8352. (b) Kutateladze, A. G.; Holt, T.; Reddy, D. S. Natural Products Containing the Oxetane and Related Moieties Present Additional Challenges for Structure Elucidation: A DU8+ Computational Case Study. *J. Org. Chem.* **2019**, *84*, 7575−7586. (c) Kutateladze, A. G.; Kuznetsov, D. M. Triquinanes and Related Sesquiterpenes Revisited Computationally: Structure Corrections of Hirsutanols B and D, Hirsutenol E, Cucumin B, Antrodins C−E, Chondroterpenes A and H, Chondrosterins C and E, Dichrocephone A, and Pethybrene. *J. Org. Chem.* **2017**, *82*, 10795−10802. (d) Novitskiy, I. M.; Kutateladze, A. G. DU8+ Computations Reveal a Common Challenge in the Structure Assignment of Natural Products Containing a Carboxylic Anhydride Moiety. *J. Org. Chem.* **2021**, *86*, 17511−17515. (e) Kutateladze, A. G.; Krenske, E. H.; Williams, C. M. Reassignments and Corroborations of Oxo-Bridged Natural Products Directed by OSE and DU8+ NMR Computation. *Angew. Chem., Int. Ed.* **2019**, *58*, 7107−7112.

(11) Kang, X.; Liang, X.; Zeng, Q. Water-Mediated Intramolecular Cyclization/Oxidation of α-Carbonyl Sulfur Ylides: Synthesis of Corey−Chaykovsky Reagent Type Heterocycles. *Org. Lett.* **2021**, *23*, 7477−7481.

(12) Ratts, K. W.; Yao, A. N. A New Rearrangement of Sulfonium Ylides. *J. Org. Chem.* **1968**, *33*, 70−75.

(13) Russell, G. A.; Kulkarni, S. V.; Khanna, R. K. Radical and Ionic Reactions of (Benzoylmethyl)mercurial. *J. Org. Chem.* **1990**, *55*, 1080−1086.

(14) Fu, Y.; Li, R.; Li, M.; Zhang, Y.; Zhang, Y.; Yang, T. Photocatalyzed Dehydroxylative Amination of Phenols: A Ring-Expansion Approach for Medium-Sized Benzolactams. *Org. Lett.* **2021**, *23*, 8317−8321.

(15) Hughes, R. O.; Li, X.; Nemoto, P. A.; Smith, K.; Lana, L.; Wu, L.; Xiong, Z. Preparation of Pyrrolidinecarboxamide Derivatives as Modulator of RORγ. WIPO Patent WO2018111803A1, 2018.

(16) Santhosh Kumar, P.; Ravikumar, B.; Ashalu, K. C.; Reddy, K. R. TBAI/TBHP mediated oxidative cross coupling of ketones with phenols and carboxylic acids: Direct access to benzofurans. *Tetrahedron Lett.* **2018**, *59*, 33−37.

(17) Xiang, L.; Kalaitzis, J. A.; Moore, B. S. EncM, a versatile enterocin biosynthetic enzyme involved in Favorskii oxidative rearrangement, aldol condensation, and heterocycle-forming reactions. *Proc. Natl. Acad. Sci. U.S.A.* **2004**, *101*, 15609−15614.

(18) Chen, Z.-H.; Tian, J.-M.; Chen, Z.-M.; Tu, Y.-Q. Total Synthesis of (±)-Parvineostemonine. *Chem. − Asian J.* **2012**, *7*, 2199−2202.

(19) Cheng, D.; Yu, C.; Pu, Y.; Xu, X. DDQ-mediated oxidative coupling reaction of N,N-dimethyl enaminones with cycloheptatriene. *Tetrahedron Lett.* **2021**, No. 153609.

(20) Zhang, C.; Qiu, Y.; Zhang, J.; Chen, L.; Xu, S.; Guo, H.; Luo, J.; Tan, Y. CAN-mediated Oxidative Coupling-Reaction of Xanthenes with Enaminones. *Asian J. Org. Chem.* **2021**, *10*, 160−163.

(21) Çelik, M.; Alp, C.; Coskun, B.; Gultekin, M. S.; Balci, M. Synthesis of diols using the hypervalent iodine(III) reagent, phenyliodine(III) bis(trifluoroacetate). *Tetrahedron Lett.* **2006**, *47*, 3659−3663.

(22) Essiz, S.; Dalkilic, E.; Sari, O.; Dastan, A.; Balci, M. Unexpected regioselectivity observed in the bromination and epoxidation reactions of p-benzoquinone-fused norbornadiene: An experimental and computational study. *Tetrahedron* **2017**, *73*, 1640−1649.

(23) Gültekin, D. D.; Taskesenligil, Y.; Dastan, A.; Balci, M. Bromination of norbornene derivatives: synthesis of brominated norbornanes and norbornenes. *Tetrahedron* **2008**, *64*, 4377−4383.

(24) (a) Reetz, M. T. Dyotropic Rearrangements, a New Class of Orbital-Symmetry Controlled Reactions. Type I. *Angew. Chem., Int. Ed.* **1972**, *11*, 129−130. For dyatropic rearrangements involving carbon-based migrating groups see (b) Leverett, C. A.; Purohit, V. C.; Johnson, A. G.; Davis, R. L.; Tantillo, D. J.; Romo, D. Dyotropic Rearrangements of Fused Tricyclic β-Lactones: Application to the Synthesis of (−)-Curcumanolide A and (−)-Curcumalactone. *J. Am. Chem. Soc.* **2012**, *134*, 13348−13356. For overview see (c) Gutierrez, O.; Tantillo, D. J. Analogies between Synthetic and Biosynthetic Reactions in Which [1,2]-Alkyl Shifts Are Combined with Other Events: Dyotropic, Schmidt, and Carbocation Rearrangements. *J. Org. Chem.* **2012**, *77*, 8845−8850.

(25) Gonzalez-de-Castro, A.; Robertson, C. M.; Xiao, J. Dehydrogenative α-Oxygenation of Ethers with an Iron Catalyst. *J. Am. Chem. Soc.* **2014**, *136*, 8350−8360.

(26) (a) It is likely that the 4-fluoro precursor was erroneously used and mislabeled as 5-fluoro. (b) Another issue complicating our analysis was that the experimental ^{13}C NMR spectrum for the starting material, pyridine **41** was attributed to structure **43** (and vice versa); it appears to be a technical error in assembling the Supporting Information section. Both starting materials are purported to have a peak at 161 ppm, which should only be found in structure **43**.

(27) Boyd, D. R.; Sharma, N. D.; Llamas, N. M.; O'Dowd, C. R.; Allen, C. C. R. syn-Benzene dioxides: chemoenzymatic synthesis from 2,3-cis-dihydrodiol derivatives of monosubstituted benzenes and their application in the synthesis of regioisomeric 1,2- and 3,4-cis-dihydrodiols and 1,4-dioxocins. *Org. Biomol. Chem.* **2007**, *5*, 2267−2273.

(28) Mattocks, A. R. Novel Reactions of Some α-Acyloxy Acid Chlorides. *J. Chem. Soc.* **1964**, 1918−1930.

(29) Note that Figure 7 presents a subset of the reactions studied in the paper.

(30) (a) Meyer, K. H.; Schuster, K. Rearrangement of tertiary ethynyl carbinols into unsaturated ketones. *Chem. Ber.* **1922**, *55*, 819−

https://doi.org/10.1021/acs.joc.2c00749
J. Org. Chem. 2022, 87, 8589−8598

823. For review see (b) Swaminathan, S.; Narayanan, K. V. The Rupe and Meyer-Schuster Rearrangements. *Chem. Rev.* **1971**, *71*, 429−438.
(31) Bovonsombat, P.; McNelis, E. Formations of Mixed *β,β*-Dihaloenals from Halogenated Secondary Alkynols. *Tetrahedron Lett.* **1992**, *33*, 7705−7708.
(32) Mahesh Kumar, K.; Khan, T.; Almansour, A. I.; Arumugam, N.; Yaragorla, S. Cyclocarbonylation-Iodination of terminal alkynes with ketones and ICl via 1,2-migration. *Tetrahedron Lett.* **2020**, *61*, No. 152374.
(33) Chen, J.-M.; Huang, X. Poly[styrene(iodosodiacetate)]-Promoted Ring Expansion Reaction of 1-Alkynylcycloalkanols: A Novel Synthesis of (Z)-2-(1-Iodo-1-organyl)-methylenecycloalkanones. *Synthesis* **2004**, 2459−2462.
(34) Aborways, M. M.; Moran, W. J. Reactions of tertiary propargyl alcohols with sodium halides under oxidative conditions. *Tetrahedron Lett.* **2014**, *55*, 2127−2129.
(35) (a) Bovonsombat, P.; McNelis, E. Ring Expansion of an *α*-Bromoalkynol Camphor by Means of Iodine and Koser's Reagent. *Tetrahedron Lett.* **1993**, *34*, 4277−4280. (b) Djuardi, E.; Bovonsombat, P.; McNelis, E. Ring Expansion of 2-Haloethynyl-2-norbornanols. *Tetrahedron* **1994**, *50*, 11793−11802.
(36) Kovacic, P.; Lowery, M. K.; Roskos, P. D. Amination of *exo*-2-chloronorbornane and norbornane with trichloroamine-aluminum chloride. *Tetrahedron* **1970**, *26*, 529−538.
(37) Alder, K.; Reubke, R. Vicinal triketones of the bicyclo[1.2.3]-octane and bicyclo[2.2.3]nonane series. A contribution to the knowledge of the reaction of Demjanov. *Chem. Ber.* **1958**, *91*, 1525−1535.
(38) Leyva, A.; Corma, A. Isolable Gold(I) Complexes Having One Low-Coordinating Ligand as Catalysts for the Selective Hydration of Substituted Alkynes at Room Temperature without Acidic Promoters. *J. Org. Chem.* **2009**, *74*, 2067−2074.
(39) (a) Goel, B.; Chatterjee, E.; Dey, B.; Tripathi, N.; Bhardwaj, N.; Khattri, A.; Guru, S. K.; Jain, S. K. Identification and Evaluation of Apoptosis-Inducing Activity of Ipomone from Ipomoea nil: A Novel, Unusual Bicyclo-[3.2.1] Octanone Containing Gibberic Acid Diterpenoid. *ACS Omega* **2021**, *6*, 8253−8260. (b) Goel, B.; Tripathi, N.; Bhardwaj, N.; Kumar, A.; Jain, S. K. Iodine-mediated one-step synthesis of ipomone from gibberellic acid. *Nat. Prod. Res.* **2022**, DOI: 10.1080/14786419.2022.2065487.

https://doi.org/10.1021/acs.joc.2c00749
J. Org. Chem. 2022, 87, 8589−8598